HHS Public Access

Author manuscript

Nat Commun. Author manuscript; available in PMC 2014 December 09.

Published in final edited form as:

Nat Commun. ; 5: 3965. doi:10.1038/ncomms4965.

An RNA Polymerase II-coupled function for histone H3K36 methylation in checkpoint activation and DSB repair

Deepak Kumar Jha[1] and **Brian D. Strahl**[1,2]

[1]Department of Biochemistry and Biophysics, School of Medicine, UNC-Chapel Hill, NC, USA

[2]Lineberger Comprehensive Cancer Center, School of Medicine, UNC-Chapel Hill, NC, USA

Abstract

Histone modifications are major determinants of DNA double-strand break (DSB) response and repair. Here we elucidate a DSB repair function for transcription-coupled Set2 methylation at H3 lysine 36 (H3K36me). Cells devoid of Set2/H3K36me are hypersensitive to DNA-damaging agents and site-specific DSBs, fail to properly activate the DNA-damage checkpoint, and show genetic interactions with DSB-sensing and repair machinery. Set2/H3K36me3 is enriched at DSBs, and loss of Set2 results in altered chromatin architecture and inappropriate resection during G1 near break sites. Surprisingly, Set2 and RNA polymerase II are programmed for destruction after DSBs in a temporal manner – resulting in H3K36me3 to H3K36me2 transition that may be linked to DSB repair. Finally, we show a requirement of Set2 in DSB repair in transcription units – thus underscoring the importance of transcription-dependent H3K36me in DSB repair.

Eukaryotic genomes are constantly subjected to exogenous and endogenous forms of DNA damage[1]. Double strand breaks (DSBs) can lead to temporary loss of genetic information, and failure to repair DSBs can lead to severe genome instability and cell death. DSBs can be programmed (e.g., meiosis and immunoglobulin rearrangements) or caused by exogenous agents (e.g., ionizing radiation (IR), ultra-violet (UV) and anti-cancer drugs)[1, 2].

In eukaryotes, chromatin plays a fundamental role in regulating the cellular response to DNA damage[2]. Among the factors that contribute to the DNA damage response (DDR) are histones and their post-translational modifications (e.g., phosphorylated H2A serine 129; γ-H2A.X in metazoans), ATP-dependent chromatin remodelers (e.g., RSC, INO80, TIP60), and histone variants (e.g., Htz1)[2]. Transcription-associated histone modifications, including H3 lysine 4 methylation (H3K4me) and H3 lysine 79 methylation (H3K79me) also contribute to DNA damage response and repair[2]. Interestingly, a majority of stalled replication sites tend to occur in transcribed genes[3], increasing the propensity for the

Corresponding author: brian_strahl@med.unc.edu.

Author contributions

D.K.J designed, performed and analyzed all the experiments, with valuable inputs from B.D.S. D.K.J and B.D.S wrote the manuscript.

Authors declare that they have no relevant conflict of interest.

collision of transcription and replication bubbles eventually resulting in DSBs[4]. Yet, how the transcription apparatus influences DSB repair is not well understood.

One major regulator of chromatin structure during transcription is H3 lysine 36 methylation (H3K36me). This mark is deposited by the Set2 methyltransferase and is highly conserved from yeast to humans[5, 6, 7, 8, 9, 10]. Set2 is recruited, at least in part, through binding to hyper-phosphorylated RNA Polymerase II (RNAPII) after RNAPII enters the productive elongation phase[5, 6, 7, 8, 9, 10]. Set2 recognizes the phosphorylated C-terminal domain (CTD) of RNAPII through the presence of a domain called the SRI domain (for Set2-RNAPII interaction domain)[7, 8]. In yeast, Set2/H3K36me regulates chromatin structure in the bodies of genes by activating the histone deacetylase complex Rpd3S[5, 11, 12, 13] and by regulating histone exchange through regulating the activity of Asf1, Chd1 and ISW1b complexes[14, 15]. Outside of a role for Set2 in transcription elongation, much less in known regarding how this enzyme contributes to other DNA-templated functions.

Here we describe a role for Set2/H3K36me in DNA repair, specifically repair of DSBs. We show that in budding yeast Set2/H3K36 is required for appropriate activation of the response to DSB as well as subsequent repair, a finding that is restricted to its function in transcription. Interestingly, we find that Set2 and RNAPII are programmed for destruction after DSBs, which for H3K36me, results in a temporal patterning of H3K36me2 and H3K36me3 around DSBs that we propose underlies the regulation of chromatin structure at break sites. Significantly, we find that Set2 loss leads to altered chromatin structure and inappropriate resection at G1 at break sites, which ultimately impacts pathway repair choice.

Results

Set2/H3K36me is required for resistance to DSB

To test whether Set2 and H3K36me function in DNA damage repair, we assessed the sensitivity of yeast cells lacking *SET2* to various genotoxic agents. Deletion of *SET2* caused sensitivity to the DSB-causing agent phleomycin (an IR-mimic), mild sensitivity to the alkylating agent methyl methane sulfonate (MMS), but no sensitivity to hydroxyurea (HU; replication stress) or UV (nucleotide damage) (Fig. 1A). The phleomycin sensitivity was rescued by transforming the *set2*Δ strain with full-length *SET2* (Fig. 1B). In contrast, sensitivity of the *set2*Δ strain could not be suppressed by transformation with a catalytically inactive *SET2* mutant ($SET2_{H199L}$); thus, methylation activity is required for survival after DSB (Figs. 1B and 1F). To further confirm the importance of Set2 in the DSB response, we utilized a strain (JKM179) in which a galactose-inducible, site-specific DSB in chromosome III can be repaired only by non-homologous end joining (NHEJ)[16] (Fig. 1C). Consistent with the phleomycin-sensitivity found with deletion of *SET2*, *set2*Δ was also sensitive to this galactose-induced DSB and was rescued by expressing wild-type (WT), but not catalytically inactive, Set2 (Figs. 1C, 1D and 1F). We ruled out the *MAT*-specific effect by using a strain with the *HO* cut site in *ADH4* gene and found that *set2*Δ was sensitive to a reparable Gal-inducible DSB as well (Supplementary Fig. 1A). Recently, it was suggested that Set2 functions in DNA damage in a catalysis-independent manner[17], however examination of the levels of H3K36me in the presumed C201A catalytic mutant used by Winsor *et. al* revealed that it only abolished the tri-methyl form of H3K36 (Supplementary Fig. 1B). Importantly,

and consistent with a role of Set2 methylation at H3K36 in this phenotype and DSB repair, we found that mutation of H3K36 (H3K36A) confers sensitivity to phleomycin (Fig. 1E).

Set2 functions through its association with the elongating (phosphorylated) form of RNAPII[7]. We therefore asked whether the DNA damage-induced phenotype we observed in the absence of Set2 and H3K36me is connected to its RNAPII function. We previously characterized a domain in the C-terminus of Set2, termed the SRI domain, which is essential for coupling Set2 with the transcribing polymerase[7]. Mutation of this domain uncouples Set2 from RNAPII and results in selective loss of H3K36me3 (Fig. 1F and[18]). Significantly, mutation of the SRI domain of *SET2* (SRIΔ) could not rescue the sensitivity of *set2*Δ to persistent gal-induced DSB (Fig. 1D). Taken together, these data suggest that Set2 functions in DSB repair through its interaction with elongating RNAPII. They further suggest the possibility that transcribing polymerase itself may play an important role in DSB repair – a finding that would be consistent with studies showing RNAPII is present at DSBs[19].

SET2 is functionally connected to DSB response and repair

To further establish that Set2 functions in cellular survival against genotoxic insults, we selected 30 genes representative of the pathways involved in DDR and repair and analyzed double mutant sensitivity to MMS. We performed our genetic interaction screen using MMS because of its ability to activate several DNA repair pathways as compared to phleomycin, thus allowing us to initially capture more possible genetic interactions between *SET2* and DDR genes. Our screen revealed that *SET2* genetically interacts (both positively and negatively) with a subset of DDR and repair genes, albeit to different extents (Fig. 2A and Supplementary Fig. 2A). In addition to recapitulating some prior genetic interactions (e.g., between *SET2* and *SLX5*) reported by the Idekker group[20], we discovered several novel genetic interactions upon MMS treatment (e.g., *RAD9* and *RAD51*) (Fig. 2A). We focused on DSB-specific genes and repeated the genetic interactions using phleomycin (examples shown in Fig. 2B and Supplementary Figs. 2A and 2B). Interestingly, the *set2*Δ*rad9*Δ double mutant was more sensitive to MMS and phleomycin than either single mutant alone, suggesting that Set2 functions in parallel to Rad9, to provide resistance to DSB (Fig. 2A, and Supplementary Fig 2C). Like the *set2*Δ single mutants, the *set2*Δ*rad9*Δ synthetic sickness was rescued by WT *SET2*, but not by a catalytically-dead version of *SET2* ($SET2_{H199L}$) (Supplementary Fig. 2C). These results agree with similar findings recently reported in a high-throughput genetic interaction map using multiple genotoxic agents[21].

Because Set2 antagonizes the histone chaperone Asf1 to regulate histone exchange during transcription elongation[15], we also asked whether the sensitivity of *set2*Δ might be due to mis-regulated histone exchange after DSB. To test this, we analyzed the *asf1*Δ*set2*Δ double mutant on phleomycin. However, the double mutant was synthetically sick on phleomycin (Fig. 2B), indicating that Set2 is required for survival in the absence of Asf1 after DSB. Our data show that in regards to DSB, Asf1 and Set2 have independent functions.

Since Set2/H3K36me is a histone modification associated with transcription elongation, we wondered whether any of the genetic interactions observed might be an indirect consequence of transcriptional alterations. However, transcription is only mildly affected in *set2*Δ[22, 23], and most of the changes are relatively modest increases in gene expression[23].

Notably, only a handful of genes are down-regulated in *set2*Δ (shown in Supplementary Table 1), and do not include any canonical DDR or repair genes. Consistent with this, the gene expression and pathway analysis performed by Lenstra *et al.* showed that *set2*Δ do not cluster with processes related to DDR and repair[23]. Additionally, we asked whether the protein levels of an early DSB response factor might be altered in *set2*Δ. We found no significant change in the proteins levels of yKu80, before or after DSB (Supplementary Fig. 1C). Thus, the specific sensitivity of *set2*Δ to DSB-causing agents is not attributable to an indirect effect of gene expression changes.

Set2/H3K36me regulates checkpoint activation after DSB

To determine if the sensitivity of *set2*Δ was due to defective DNA-damage signaling, we exposed asynchronous cultures of WT and *set2*Δ strains to either MMS (M) or phleomycin (P) and monitored activation of γ-H2A.X (or H2AS129ph) and Rad53 (yeast homolog of mammalian Chk2). We observed reduced levels of Rad53 activation and γ-H2A.X in *set2*Δ, suggesting attenuated DSB damage response signaling (Figs. 3A, 3B and Supplementary Fig. 3B). Deletion of *SET2* in the evolutionarily divergent yeast species *Schizosaccharomyces pombe* also resulted in reduced H2AS129ph when exposed to phleomycin (Supplementary Fig. 3A).

γ-H2A.X activation is one of the earliest steps after DSB-induction and occurs with extremely fast kinetics[24]. To determine if this reduced level of γ-H2A.X was due to inefficient activation or faster de-phosphorylation (which normally occurs later in the DDR pathway)[25], we monitored the activation of γ-H2A.X after DSB-induction by phleomycin. We observed significantly lower levels of γ-H2A.X within the first hour of phleomycin treatment of *set2*Δ cells (Fig. 3C), implying a function for Set2 at an early step after DSB. Additionally, and in line with reduced activation of DNA damage checkpoint, Rad53 hyper-phosphorylation was severely reduced in a *set2*Δ strain in a similar time-scale (Fig. 3D). Importantly, we found Rad53 activation was also reduced in a H3K36A strain (Fig. 3E). Taken together, our data show that Set2-mediated H3K36me is essential for maximal activation of the DNA damage checkpoint after DSB induction.

H3K36me2 and me3 are DSB-inducible and present at DSBs

Because the catalytic function of Set2 is responsible for providing resistance to DSBs (Fig. 1) and full activation of DDR (Fig. 3), we next determined if the levels of H3K36me change after induction of DSB. We induced DSBs using phleomycin in an asynchronously growing culture and monitored H3K36me3 levels by Western blot analysis. Interestingly, H3K36me3 levels increased globally within an hour after exposure to phleomycin and then returned to basal levels (Fig. 4A). In contrast, H3K36me2 increased with much slower kinetics (Fig. 4B) and reached its highest levels at a later time-point (i.e., 4-5 hours after phleomycin treatment). Although it is possible that the increase in H3K36me2 at the later time-point was an active response to DSB, the increase coincided with the decrease in H3K36me3 – suggesting a specific loss of H3K36me3 to form more H3K36me2. To further verify that we were monitoring a DSB-inducible histone modification, we examined the levels of H3K36me3 near the site of DSB (0.2 kb distal to the DSB in the *MAT* locus) at early time-points to accurately capture a transient induction. H3K36me3 was increased, although

modestly, within 30 minutes of galactose-induced DSB and tapered off approximately 75 minutes after DSB induction (Fig. 4C). This degree of increase is in line with the changes reported for H4 acetylation around the DSB[26, 27]. Consistent with global H3K36me2 levels measured by immunoblot (Fig. 4B), ChIP analysis indicated that H3K36me2 was induced at a later time point than H3K36me3 (Fig. 4D). Further, we detected an enrichment of Set2 at the DSB at an early time-point following DNA damage (Fig. 4E). The specificities of our H3K36me3, H3K36me2 and Set2 antibodies were confirmed by inclusion of a *set2*Δ sample (Figs. 4A-E and Supplementary Fig. 4). Collectively, our data indicates H3K36me3 is DSB-inducible and transitions into H3K36me2 – a finding which coincides with transiently enriched Set2.

To further understand the molecular basis for the temporal regulation of H3K36me2 and H3K36me3, we monitored the global levels of Set2 following DNA damage. Upon MMS and phleomycin treatment, we found that Set2 protein levels were significantly decreased (Fig. 4F). Surprisingly, we also noticed that the levels of Rpb1 (the largest subunit of RNAPII), and consequently the Ser2 phosphorylated form of RNAPII CTD (Ser2p CTD), also degraded after DNA damage in a proteasome-dependent manner (Fig. 4F and Supplementary Figs. 4B, 4F). Collectively, these results reveal a programed destruction of Set2 and RNAPII after DSB, which may be an important event in DSB sensing and repair.

To monitor if we see a similar reduction in the levels of RNAPII in the vicinity of a DSB, we did ChIP analysis for RNAPII around the *MAT* DSB. Consistent with the presence of Set2, we see RNAPII to be present at the same locus. Additionally, after 30 minutes of DSB induction, we can see significant reduction in the level of RNAPII (Supplementary Figure 4G), a result consistent with our global analysis. To our knowledge, this is the first demonstration of proteasome-dependent regulation of RNAPII after DSB in any model system.

To further understand how Set2 is regulated after DSB, we immunoprecipitated FLAG-tagged Set2 at several time-points following phleomycin treatment. We noticed an increase in pS/T-phosphorylation (a mark commonly associated with phosphorylation-dependent degradation[28]) concomitant with reduced Set2 levels (Supplementary Fig. 4D). While Set2 degradation is likely attributed to loss of RNAPII interaction, an alternate hypothesis could be that Set2 is targeted for phosphorylation-dependent degradation in a checkpoint-dependent manner after DSB. However, we found that Set2 levels were still decreased in a number of key checkpoint mutants tested (Supplementary Fig. 4E). These data show that in WT cells, Set2, RNAPII and H3K36me are regulated after DSB, consistent with a role for Set2/H3K36me in regulating cellular resistance to DSB.

Interplay between Set2 and chromatin regulators after DSB

Our genetic and biochemical evidence suggests that Set2 has a methylation- and RNAPII-dependent function after DSB. Set2-catalyzed H3K36me modulates chromatin structure via activation of the Rpd3S histone deacetylase complex[5, 11, 12, 13], antagonizing the function of Asf1[15] and regulating ISW1b function[14]. Thus, we investigated whether any of these pathways contribute to the function of Set2 after DSB. As mentioned above, the *asf1*Δ*set2*Δ double mutant is synthetically sick on phleomycin, suggesting that Set2 and Asf1 function in

parallel after DSB (Fig. 2B). Consistent with this finding, we also noticed synthetic sickness of H3K36A with H3K56R (H3K56Ac being a marker of histone exchange) on phleomycin (Supplementary Fig. 2E). To test the other possible H3K36me effector proteins, we deleted *RCO1* (Rpd3S-specific subunit), *IOC4* (Isw1b-specific H3K36me effector protein) and *YLR455w* (a PWWP-containing putative H3K36me binder) and determined if any of these strains phenocopied *set2*Δ. None of these known or putative H3K36me effector proteins showed similar phleomycin sensitivity as *set2*Δ in isolation (Supplementary Fig. 2D). Whether specific combinations of these effectors are required or if a novel effector protein is reading H3K36me remains to be determined.

We next investigated other histone modifiers known to play a role in the DDR, Dot1 and the histone variant Htz1. Dot1-dependent H3K79 methylation (H3K79me) and Htz1 are two chromatin components that are crucial for DSB response and repair[29, 30, 31, 32, 33, 34]. H3K79me modulates the DSB checkpoint response by recruiting or stabilizing the Rad9 adaptor protein on chromatin[34, 35] and inhibits DSB end-resection in a Rad9-dependent fashion[36, 37]. Htz1 has been implicated in a multitude of events occurring after DSB. We investigated the genetic interactions between *SET2* with *DOT1* and *HTZ1* to determine whether Set2 is part of any of the known pathways (or processes) in which these proteins function after DSB. We observed that *set2*Δ was synthetically sick with *htz1*Δ and *swr1*Δ (Supplementary Fig. 2E), but *set2*Δ suppressed the mild resistance of *dot1*Δ to phleomycin (Fig. 2B). These data reveal that Set2/H3K36me is required for cell survival in the absence of Swr1/Htz1 function. They also suggest that Set2 and Dot1 might function in antagonistic manner to regulate cellular response to DSB.

Set2 regulates chromatin dynamics around a DSB

Based upon synthetic sickness of *set2*Δ with genes involved in homologous recombination, early abrogation of DNA damage checkpoint and sensitivity to ‘error-prone NHEJ’ (as revealed by persistent DSB in JKM179 ‘donor-less’ strain) (Fig.1C), we investigated if the early steps of chromatin remodeling might be defective in cells deleted for *SET2*. Thus, we induced DSB (in asynchronous cultures) by galactose treatment in the JKM179 donor-less strain and performed a time-course-based ChIP experiment for histones, their post-translational modifications and histone variants, at regions near the DSB and at an unrelated locus (ARS315) as a control. We monitored the DSB induction kinetics, using primers across the induced DSB, in WT and s*et2*Δ and found that to be identical (Supplementary Fig. 5a). We also confirmed the reduced DNA damage checkpoint activation in *set2*Δ by monitoring γ-H2A.X around a DSB. Consistent with previously published results for γ-H2A.X around a DSB, we observed a rapid accumulation of γ-H2A.X within an hour of DSB induction. In contrast, *set2*Δ showed no significant γ-H2A.X activation (Fig. 5A).

After a DSB, an early response of WT cells is to ensure a de-acetylated chromatin state, thereby enabling NHEJ in yKu70-80-dependent fashion[38, 39, 40, 41]. Removal of yKu70-80, due to activation of Sae2 (and other resection enzymes) results in DSB being processed for homologous recombination[41], which correlates with increased acetylation of histones[26, 27]. Consistent with previously published results for H4 acetylation[38], in WT cells, H4 acetylation decreased early, followed by an increase in H4 acetylation (Fig. 5B, solid line, at

0.2kb away from DSB). In contrast, H4 acetylation was significantly higher in *set2*Δ cells compared to WT cells around 1.5 hour after gal-induced DSB (Fig. 5B, dashed line). Notably, the subsequent increase in H4 acetylation seen in WT cells did not occur in *set2*Δ cells (Fig. 5B, dashed line), indicating that the dynamic changes in H4 acetylation that normally occur after a DSB were altered in the absence of Set2 – a result consistent with the idea that chromatin structure at DSBs is influenced by Set2 and H3K36me. Because NuA4 drives, in large part, H4 acetylation at DSBs, the altered H4 acetylation seen in *set2*Δ cells may have been due to altered NuA4 activity (a result also consistent with the finding that NuA4 function is partially depended on H3K36me[42]).

Given the observed changes in H4 acetylation, we next looked at Htz1, an H2A histone variant that is deposited at DSBs by the SWR1 complex, which recognizes acetylated histones[43, 44, 45]. Consistent with published literature, Htz1 levels decreased in the vicinity of the DSB in WT cells (Fig. 5C)[2]. In contrast, there was more retention of both Htz1 and H3 around the same DSB in *set2*Δ cells (Figs. 5C and Supplementary Fig. 5B). The level of Htz1 was not altered globally (Supplementary Figure 5F). Aberrant retention of Htz1-containing nucleosomes around the DSB reduces the available biochemical pool of substrate for Tel1 (i.e., H2A) and this may provide a molecular basis for the defects in the DNA damage checkpoint that is observed in the absence of Set2 (i.e., reduced γ-H2A.X) (Figs. 3 and 6), although we formally do not rule out an abrogated activation of Tel1 as a molecular explanation. However, a similar antagonistic relationship has been observed in the case of *ino80*Δ (chromatin remodeling complex required for removing Htz1 from chromatin), where increased retention of Htz1 reduces γ-H2A.X [31].

Given the critical role nucleosomal architecture plays in DSB response and the known role of FACT, a major regulator of nucleosome structure, in cellular resistance to DSBs in mammalian cells[46], we next investigated if *SET2* functionally interacts with the FACT complex. Interestingly, the Spt16 subunit of FACT regulates H2A.X exchange at DSBs in human cells, indicating that FACT regulates nucleosome dynamics at DSBs. In yeast, mutants of Spt16 (e.g., *spt16-11*) are sensitive to replication stress and high temperature and significantly, are suppressed by deletion of *SET2*[47, 48]. We therefore reasoned that FACT mutants may be sensitive to genotoxic agents and this genotoxic sensitivity would be suppressed by *set2*Δ. As shown in Supplementary Fig. 5C, we found that the *spt16-11* allele was extremely sensitive to phleomycin at permissive temperature. Consistent with the idea that Set2 opposes the action of FACT function[48], deletion of *SET2* suppressed, albeit partially, the DSB sensitivity of the *spt16-11* strain. These data suggest the intriguing possibility that Set2 and FACT have opposing effects on nucleosomal dynamics at DSBs.

Set2 regulates DSB repair in the context of transcription

We next asked what the functional consequence of losing Set2 and H3K36me would be on DNA repair and repair pathway choice. Our data show that loss of Set2/H3K36me results in aberrant retention of Htz1-containing nucleosomes at DSBs, suggesting an unstable nucleosome architecture around these regions since Htz1-containing nucleosomes result in less stable nucleosomes[49]. Importantly, a recent study showed that Htz1-containing nucleosomes aid in Exo1-dependent end-resection[50]. We therefore used the input DNA from

our cycling cells and monitored the loss of input DNA (as a surrogate readout of end resection). We did not detect any difference in the rate of input DNA loss compared to that of *set2*Δ cells (Supplementary Fig. 5D). However, end-resection is heavily influenced by the cell cycle (G1 vs. G2/M), and smaller differences in resection kinetics may not become apparent in cycling cells. Therefore, we arrested cells in G1 by α-factor and monitored the loss of input DNA. In WT cells, we did not see any significant loss in input DNA, but, in *set2*Δ cells, the input DNA was rapidly lost, suggesting that *set2*Δ cells show faster end-processing in G1-arrested cells – a time when resection is normally suppressed (Fig. 5D). We confirmed this by monitoring the enrichment of single-strand DNA binding protein, RPA, in G1-arrested cells. We observed that even within 30 minutes after DSB induction, there is more RPA around a DSB in a *set2*Δ as compared to WT (Supplementary Fig. 6A and 6B). This effect is likely a direct consequence of having more Htz1-containing nucleosomes in a *set2*Δ as well as reduced γ-H2A.X, which is known to be inhibitory to resection[37].

One prediction from this observation would be that Set2 should regulate non-homologous end-joining (NHEJ), and in the absence of Set2, one should see lower end-joining efficiency. A canonical assay used to monitor the efficiency of end-joining is the calculation of the ratio of colony numbers obtained after transformation of linearized plasmids to that obtained from transforming a circular plasmid (i.e., re-ligation efficiency). Using a plasmid where we generated a blunt-end cut in the plasmid multiple cloning site, we observed that there was no difference in the re-ligation efficiency between WT and *set2*Δ strains (Fig. 6A). However, since Set2 functions in the context of transcription units, we hypothesized that the function of Set2 in DNA repair would be more evident if our cut site was in the context of a gene body. We therefore carried out the plasmid religation assay again, but in this case, with the cut site within the LacZ gene body. Strikingly, we observed a significant increase in plasmid re-ligation efficiency in *set2*Δ strains (Fig. 6B). We take these results to mean that although Set2 regulates pathway choice with a likely preference towards promoting NHEJ, the loss of Set2 does not completely ablate this function – hence, some plasmid would be re-ligated that would then serve as a template for ensuing HR as the balance has been tilted to this pathway. Importantly, HR is a canonical mechanism of repair in transcription units[51, 52], which would further exacerbate the *set2*Δ phenotype resulting in more re-ligation.

We next asked if this increased re-ligation efficiency is indeed a consequence of more recombination events, presumably due to transcription[51]. To answer that question, we deleted *RAD51* in *set2*Δ and monitored the re-ligation efficiency. Consistent with the idea proposed above, we observed that the increase in plasmid re-ligation efficiency in a *set2*Δ was suppressed by deletion of *RAD51* (Fig. 6B), indicating that *set2*Δ cells exhibit increased HR. To investigate if this effect was specific for the type of DSB induced, we used another restriction enzyme (SacI) that creates staggered ends, again in the context of transcription. Even in this context, we observed higher plasmid re-ligation efficiency in *set2*Δ strains (Supplementary Fig. 6C). This phenotype of *set2*Δ is reminiscent of *rsc* and *sth1* mutants, where linearization of the plasmid by digestion in a transcription unit resulted in higher re-ligation efficiency than wild-type cells[53]. Although the precise mechanism of increased re-

ligation efficiency is not yet understood, these results reinforce the idea that Set2/H3K36me plays an important role in DSB repair, especially in the context of transcription.

Discussion

In this article, we provide genetic and biochemical evidence that Set2, and its methylation at H3K36, functions at an early step after DSB and plays a role in DSB repair. Specifically, we find Set2/H3K36me is critical for proper DSB checkpoint activation and impinges on pathway choice – results that can be linked to its function with elongating RNAPII. The role of Set2/H3K36me in DDR and repair is likely to maintain appropriate chromatin structure at break sites, which impinges on the molecular events that occur during DNA repair.

Our data provide a temporal picture of how Set2 and H3K36me might modulate chromatin structure after a DSB. Using time-course immunoblotting and ChIP, we found that loss of Set2 leads to reduced γ-H2A.X, increased acetylation of H4 and aberrant retention of H3 and Htz1 at break sites. We propose that this altered chromatin architecture underlies the increased end-resection observed in G1-arrested cells, suggesting that HR is activated sooner in *set2*Δ at G1. Additionally, we found that loss of Set2 leads to increased HR, when a DSB is in the gene body. Future experiments will be required to determine if H3K36me3 or H3K36me2 plays an important role in recruiting any DSB repair factors to control repair pathway choice, in a cell-cycle and/or transcription-dependent manner. Although H3K36me2 affects Ku70-80 recruitment to DSB in human cells[54], such recruitment appears not to occur in cycling yeast cells as we did not see any significant alterations in Ku80 recruitment in *set2*Δ (Supplementary Fig. 5E).

We found that Set2 and RNAPII are programmed for destruction after DSBs in a proteasome-dependent manner, which correlates with a transition of H3K36me3 to H3K36me2 (Figs. 4 and Supplementary Figure 4). Although the function of this transition in DSB repair is not yet known, we hypothesize that this methyl-state transition after DSB functions to ensure a chromatin structure that is temporally ‘tunable’ for DSB repair. We speculate that the fine-tuning of chromatin structure via H3K36me states would come from the ability of these different methyl states to activate/regulate functions of HATs and HDACs[55].

With regards to Htz1, the dynamic level of Htz1 around a DSB is critical for multiple steps in the response to DSB. Intriguingly, both *in vivo* and *in vitro*, H3K36me3 and Htz1 are mutually exclusive[56, 57]; hence, one function of an early increase in H3K36me3 at sites of DSBs could be to prevent Htz1 deposition, thereby allowing more H2A (H2A and Htz1 being mutually exclusive in chromatin) to be phosphorylated to form γ-H2A.X domains. Consistent with this idea, we observed increases in Htz1 and lower γ-H2A.X in a *set2*Δ (Figs. 3 and 5).

Our study found that Set2’s function in DDR and repair is dependent on its association with elongating RNAPII (Fig. 1). Consistent with this, we observed that when a DSB is in the context of transcription, deletion of *SET2* leads to an increase in HR events (Fig. 6). This result might be explained by the fact that Set2 loss tips the balance away from NHEJ to HR,

which can be a preferred mechanism for break site repair in transcription units. We speculate that Set2-dependent chromatin compaction in G1 aids in preventing HR events, which would further prevent inappropriate recombination events that would arise in genes at this point in the cell cycle. It is also interesting to note that Set2/H3K36me is correlated with transcription rates and gene lengths[15] – which might fine-tune the appropriate type of repair that would occur in genes undergoing distinct rates of transcription.

The dependence of Set2/H3K36me for proper repair in gene bodies provides further evidence for an RNAPII–dependent DNA damage sensing mechanism. Lindsey-Boltz and Sancar postulated the existence of such a DNA damage 'sensor' due to the extremely slow off-rate of RNAPII on DNA[58]. Consistent with this idea, studies (including these herein) have found RNAPII at sites of DSB in yeast (and mammals)[19] and NuA4 and other chromatin modifiers that associate and function at DSBs are also associated with RNAPII[2]. In mammalian cells, DSB induces local chromatin silencing if the DSB is in a gene body. We surmise that the transcription machinery can be "co-opted" by the DNA repair and signaling machinery to sense DNA damage and then use the already available chromatin modifiers (ATP-dependent remodelers/histone variants) to access and repair the damage, followed by restoration of the chromatin structure. This scenario would be especially useful during gene transcription induced R-loop formation, which can result in single or double-strand breaks[59]. Interestingly, both transcription and DSBs result in fairly identical mitotic recombination events[52], making the possibility of RNAPII as a 'constitutive DSB sensor' even more plausible[58]. Given the stochastic nature of transcription[60], using the transcription apparatus as a sensor for DNA damage can be a useful strategy for cells to rapidly respond to exogenous or endogenous genomic insults. Consistent with this model, a recent paper by the Legube group[61] shows that transcription units preferentially shunt the DSB to HR dependent pathways. This phenomenon also was dependent upon the presence of the mammalian Set2 homolog, SETD2, and presence of H3K36me3. We speculate that the DSB repair machinery can utilize the context-dependent chromatin environment to access and repair the DSB and maintain genome integrity.

Finally, the conservation of H3K36me across different species lends credibility to the idea that H3K36me is also important for DSB repair and damage response in other organisms. Indeed, Tim Humphrey's group has discovered that the *S. pombe* Set2 also regulates pathway choice, because deletion of *SET2* alters the balance between NHEJ and HR[**62**]. Interestingly, they find that Gcn5 acetylates H3K36[63] when Set2 is absent, and this activity leads to increased HR by presumably making the chromatin more accessible to the HR pathway. Additionally, Fnu *et al.* showed that H3K36me2 catalyzed by SETMAR/Metnase, which is not a canonical H3K36 methyltransferase, is critical for NHEJ in human cells[54]. Taken together, we propose Set2 as a key player in the DNA repair pathway that likely impinges on genome stability. As human SETD2[64] is mutated in a variety of cancers[65], we speculate that SETD2 has a conserved role in DNA repair that would explain its connection to human disease.

Materials and Methods

Yeast Strains and Plasmids

All strains, unless otherwise stated, were in the BY4741 background. The strain for *GAL*-inducible Homothallic endonuclease (*HO* endonuclease; JKM179) was obtained from James Haber, Brandeis University and subsequent gene deletions (*SET2* and *YKU70*) were performed by gene replacement using the PCR tool kit.

Plasmids expressing *SET2* from its own promoter were obtained from Scott Briggs (Purdue University) and the H199L mutation was made in full length *SET2* by site directed mutagenesis (Quikchange, Stratagene).

DNA damage Sensitivity Assays

Cultures grown overnight were diluted to an OD_{600} of 0.25, 5-fold serially diluted, and spotted on plates with or without relevant drugs. For UV experiments, cells were spotted on control plates and exposed to a range of UV dosage (from 20-60J/m^2 in Stratagene cross-linker P1800, *rad4*Δ served as a positive control for sensitivity to UV). For *GAL*-inducible DSB, overnight grown cells were serially diluted (starting ODs of between 2 and 5) as indicated above and spotted on Sc-Ura plates containing either 2% dextrose or 2% galactose. Pictures were taken after 2-4 days. For liquid culture experiments, log phase cultures were exposed to phleomycin (250 μg/mL except for Fig. 3b, wherein 50 μg/mL was used to test whether the phenotype was due to a high concentration of phleomycin) for indicated times, and then extracts were prepared by SUMEB method. About 5 O.D equivalent of cells were taken and lysed by bead beating using the lysis buffer containing (1% SDS, 8M Urea, 10mM MOPS, pH 6.8, 10mM EDTA, 0.01% bromophenol blue). 200 μL of buffer with 200 μL equivalent of glass beads were used to lyse the cells. Bead beating was done for 6-8 minutes, intermittently, and the extracts were centrifuged, to clarify, and boiled at 95 °C for 5 minutes before loading the SDS-PAGE gel.

Whole Cell Protein Extract and Immunoblots—Asynchronously grown mid-log (0.6-0.8 OD) phase cultures were lysed by SUMEB using glass beads, as mentioned above. For histones, 15% SDS-PAGE gels were run using Laemmli buffer. For Set2, RNA Polymerase II and Rad53 blots, 8% SDS-PAGE gels were run. Gels were transferred using a semi-dry Hoeffer apparatus at 45mA/gel (constant current setting), 50V for 1.5 hours. For RNA Polymerase II, the Hoeffer setting was 55mA/gel (constant current setting), 50V for 1.5hours. Primary antibodies were incubated in 5% milk over night and secondary antibodies were incubated in 5% milk for an hour. The immunoblots were developed using ECL-Prime from Amersham. An un-cropped version of major immunoblots can be found in the Supplementary Figure 7. Antibodies: H3K36me1 (ab9048; 1:1000); H3K36me2 (active motif 39255; 1:1000 and 4μL for ChIP), H3K36me3 (ab9050; 1:10, 000 and 3μL for ChIP), C-terminal H3 (EpiCypher 13-0001; 1:2500 and 2μL for ChIP), Set2 (raised in lab; 1:5000 or 1:10,000 and 5μL for ChIP), Rad53 (obtained from Daniel Durocher, Canada; 1:2000 (for Figure 3A[66]) and Abcam 104232; 1:2000 (for all other Rad53 blots), H2AS129ph (Active Motif 39271; 1:1000 and 2μL for ChIP), H2A (Active Motif 39235; 1:25,000 and 2μL for ChIP), G6PDH (Sigma; 1:100,000), Ser2pCTD (1:100, gift from Dirk Eick, LMU– Munich,

Germany), Rpb1 (Santa Cruz, yN-18, 1:1000), anti-Myc (9E10, 1:2500), 4H8 against RNA Polymerase II (Active Motif; 1:10,000 and 4 μL for ChIP). Rabbit (Amersham, Donkey anti-Rabbit), Goat and Rat (both Jackson ImmunoResearch Laboratories) secondary antibodies was used at 1:10,000. RPA antibody (2μL for about 1mg of chromatin) from Valerie Borde (Insitut Pasteur, Paris) was used for ChIP in Supplementary Figure 6.

ChIP

JKM179 and derivatives thereof were grown over night in YPD and the saturated culture was used to start a fresh culture in YEP lactate, pH 5.5 (SC-Ura plus 2% Sucrose for figure 5D) at an OD_{600} of 0.1 and grown at 30°C till the OD_{600} reached 0.8-1.0. Galactose was added to a final concentration of 2% to induce the expression of homothallic endonuclease (*HO*) (at t=0 hour). Samples were collected at required time-points and fixed with 1% (final concentration) formaldehyde. Cells were lysed using 300mM FA lysis buffer (containing protease inhibitor cocktail). The lysed cells were sonicated (30% output, 6 pulses 6 times; 90% duty cycle) and clarified by centrifuging at full speed for 15 minutes. Immuno-precipitations were set-up, overnight, with desired amount of proteins and antibodies (antibody amounts have been listed above). Protein G-sepharose beads (100 μL 1:10 diluted beads per 400 μL immunoprecipitation reaction) were added to the immuno-precipitation reactions and the reactions were allowed to incubate for one hour. Subsequent washes were done in 1.4 mL of 300mM FA Lysis buffer, 500mM FA-lysis buffer and LiCl solution (250mM LiCl, 10mM Tris, 0.5% each of NP-40 and sodium deoxycholate and 1mM EDTA). The immunoprecipitates were resuspended in TE, pH 8.0 and was treated with RNase for 30 minutes. The immunoprecipitates were then washed with TE pH 8.0 and elution buffer was used to elute the DNA (15 minutes incubation in elution buffer followed by centrifugation at 3000 rpm for two minutes). The eluates were kept at 65°C overnight to carry out the de-crosslinking step and PCR purification kit (Qiagen) was used to extract the DNA. Details of PCR conditions, primer locations and analysis methodologies can be found in the supplementary methods.

Immunoprecipitation

Immunoprecipitation for Set2-FLAG was performed in accordance with manufacturer's protocol (SIGMA, catalog no. A2220), using the 300mM FA-lysis buffer used for ChIP experiments.

MG-132 experiment

Cells were grown in media containing proline as a nitrogen source overnight. The following morning, a fresh culture was started at OD 0.5 with 0.003% SDS and grown for 3 hours before treatment with MG-132 (75 μM) for another 30 minutes. Subsequently, phleomycin (250 μg/mL) was added and samples were obtained at indicated times and western blotting were done as described above.

Plasmid Religation Assay

About 3-5 μg of circular plasmids were digested by indicated restriction enzymes. Running the digested plasmids on gels and performing routine gel extraction confirmed their

linearization. Subsequently, 100ng of linearized or circularized plasmids were transformed into indicated strains (LiAc/PEG method), in parallel. The colonies were counted on Sc-Ura plates after 2-3 days. Three independent transformation reactions were carried out.

Statistical Analysis

For arriving at the p-values in all the relevant experiments (ChIP assays and the plasmid re-ligation assay), we carried out unpaired Student's t-test in Microsoft Excel. The explanations for the error bars are mentioned in the corresponding figure legends with relevant n-values. $p < 0.05$ was considered statistically significant.

Supplementary Material

Refer to Web version on PubMed Central for supplementary material.

Acknowledgements

We thank James Haber (Brandeis University) for JKM179 strain and valuable suggestions, Daniel Durocher (University of Toronto) for Rad53 antibody used in parts of Fig. 3, Marcus Smolka (Cornell University) for suggesting the Abcam Rad53 antibody (used in parts of Fig. 3), Ugur Yavuzer (Bilkent University, Turkey; for the plasmids used in Figure 6B and Supplementary Figure 6C), Katsunori Sugimoto (University of Medicine and Dentistry New Jersey; for the ADH4-HO strain used in Supplementary Figure 1A), Valerie Borde (Institut Curie, Paris) for the RPA antibody and suggestions for RPA chip and Scott Briggs for the full-length and the SRIΔ *SET2* plasmid. We thank Timothy Humphrey (Oxford University) for communicating results prior to publication. We are thankful to Jean Cook, Lindsay Faircloth Rizzardi, Zu-Wen Sun, Howard Fried and members of the Strahl lab, especially Raghuvar Dronamraju (for helpful suggestions) and Stephen McDaniel (for some of the unpublished strains). This work was funded by a NIH grant to B.D.S (GM068088).

References

1. Hoeijmakers JH. DNA damage, aging, and cancer. N Engl J Med. 2009; 361:1475–1485. [PubMed: 19812404]
2. Papamichos-Chronakis M, Peterson CL. Chromatin and the genome integrity network. Nat Rev Genet. 2013; 14:62–75. [PubMed: 23247436]
3. Azvolinsky A, Giresi PG, Lieb JD, Zakian VA. Highly transcribed RNA polymerase II genes are impediments to replication fork progression in Saccharomyces cerevisiae. Mol Cell. 2009; 34:722–734. [PubMed: 19560424]
4. Bermejo R, Lai MS, Foiani M. Preventing replication stress to maintain genome stability: resolving conflicts between replication and transcription. Mol Cell. 2012; 45:710–718. [PubMed: 22464441]
5. Keogh MC, et al. Cotranscriptional set2 methylation of histone H3 lysine 36 recruits a repressive Rpd3 complex. Cell. 2005; 123:593–605. [PubMed: 16286008]
6. Strahl BD, et al. Set2 is a nucleosomal histone H3-selective methyltransferase that mediates transcriptional repression. Mol Cell Biol. 2002; 22:1298–1306. [PubMed: 11839797]
7. Kizer KO, Phatnani HP, Shibata Y, Hall H, Greenleaf AL, Strahl BD. A novel domain in Set2 mediates RNA polymerase II interaction and couples histone H3 K36 methylation with transcript elongation. Mol Cell Biol. 2005; 25:3305–3316. [PubMed: 15798214]
8. Xiao T, et al. Phosphorylation of RNA polymerase II CTD regulates H3 methylation in yeast. Genes Dev. 2003; 17:654–663. [PubMed: 12629047]
9. Wagner EJ, Carpenter PB. Understanding the language of Lys36 methylation at histone H3. Nat Rev Mol Cell Biol. 2012; 13:115–126. [PubMed: 22266761]
10. Li B, Howe L, Anderson S, Yates JR 3rd, Workman JL. The Set2 histone methyltransferase functions through the phosphorylated carboxyl-terminal domain of RNA polymerase II. J Biol Chem. 2003; 278:8897–8903. [PubMed: 12511561]

11. Carrozza MJ, et al. Histone H3 methylation by Set2 directs deacetylation of coding regions by Rpd3S to suppress spurious intragenic transcription. Cell. 2005; 123:581–592. [PubMed: 16286007]
12. Joshi AA, Struhl K. Eaf3 chromodomain interaction with methylated H3-K36 links histone deacetylation to Pol II elongation. Mol Cell. 2005; 20:971–978. [PubMed: 16364921]
13. Govind CK, et al. Phosphorylated Pol II CTD recruits multiple HDACs, including Rpd3C(S), for methylation-dependent deacetylation of ORF nucleosomes. Mol Cell. 2010; 39:234–246. [PubMed: 20670892]
14. Smolle M, et al. Chromatin remodelers Isw1 and Chd1 maintain chromatin structure during transcription by preventing histone exchange. Nat Struct Mol Biol. 2012; 19:884–892. [PubMed: 22922743]
15. Venkatesh S, et al. Set2 methylation of histone H3 lysine 36 suppresses histone exchange on transcribed genes. Nature. 2012; 489:452–455. [PubMed: 22914091]
16. Moore JK, Haber JE. Cell cycle and genetic requirements of two pathways of nonhomologous end-joining repair of double-strand breaks in Saccharomyces cerevisiae. Mol Cell Biol. 1996; 16:2164–2173. [PubMed: 8628283]
17. Winsor TS, Bartkowiak B, Bennett CB, Greenleaf AL. A DNA damage response system associated with the phosphoCTD of elongating RNA polymerase II. PLoS One. 2013; 8:e60909. [PubMed: 23613755]
18. Youdell ML, et al. Roles for Ctk1 and Spt6 in regulating the different methylation states of histone H3 lysine 36. Mol Cell Biol. 2008; 28:4915–4926. [PubMed: 18541663]
19. Tsukuda T, Fleming AB, Nickoloff JA, Osley MA. Chromatin remodelling at a DNA double-strand break site in Saccharomyces cerevisiae. Nature. 2005; 438:379–383. [PubMed: 16292314]
20. Bandyopadhyay S, et al. Rewiring of genetic networks in response to DNA damage. Science. 2010; 330:1385–1389. [PubMed: 21127252]
21. Guenole A, et al. Dissection of DNA damage responses using multiconditional genetic interaction maps. Mol Cell. 2013; 49:346–358. [PubMed: 23273983]
22. Tompa R, Madhani HD. Histone H3 lysine 36 methylation antagonizes silencing in Saccharomyces cerevisiae independently of the Rpd3S histone deacetylase complex. Genetics. 2007; 175:585–593. [PubMed: 17179083]
23. Lenstra TL, et al. The specificity and topology of chromatin interaction pathways in yeast. Mol Cell. 2011; 42:536–549. [PubMed: 21596317]
24. Shroff R, et al. Distribution and dynamics of chromatin modification induced by a defined DNA double-strand break. Curr Biol. 2004; 14:1703–1711. [PubMed: 15458641]
25. Keogh MC, et al. A phosphatase complex that dephosphorylates gammaH2AX regulates DNA damage checkpoint recovery. Nature. 2006; 439:497–501. [PubMed: 16299494]
26. Tamburini BA, Tyler JK. Localized histone acetylation and deacetylation triggered by the homologous recombination pathway of double-strand DNA repair. Mol Cell Biol. 2005; 25:4903–4913. [PubMed: 15923609]
27. Lin YY, et al. A comprehensive synthetic genetic interaction network governing yeast histone acetylation and deacetylation. Genes Dev. 2008; 22:2062–2074. [PubMed: 18676811]
28. Warmerdam DO, Kanaar R. Dealing with DNA damage: relationships between checkpoint and repair pathways. Mutat Res. 2010; 704:2–11. [PubMed: 20006736]
29. Kalocsay M, Hiller NJ, Jentsch S. Chromosome-wide Rad51 spreading and SUMO-H2A.Z-dependent chromosome fixation in response to a persistent DNA double-strand break. Mol Cell. 2009; 33:335–343. [PubMed: 19217407]
30. Lazzaro F, et al. Histone methyltransferase Dot1 and Rad9 inhibit singlestranded DNA accumulation at DSBs and uncapped telomeres. Embo J. 2008; 27:1502–1512. [PubMed: 18418382]
31. Papamichos-Chronakis M, Krebs JE, Peterson CL. Interplay between Ino80 and Swr1 chromatin remodeling enzymes regulates cell cycle checkpoint adaptation in response to DNA damage. Genes & development. 2006; 20:2437–2449. [PubMed: 16951256]

32. van Attikum H, Fritsch O, Gasser SM. Distinct roles for SWR1 and INO80 chromatin remodeling complexes at chromosomal double-strand breaks. Embo J. 2007; 26:4113–4125. [PubMed: 17762868]
33. Wysocki R, Javaheri A, Allard S, Sha F, Cote J, Kron SJ. Role of Dot1-dependent histone H3 methylation in G1 and S phase DNA damage checkpoint functions of Rad9. Mol Cell Biol. 2005; 25:8430–8443. [PubMed: 16166626]
34. Grenon M, et al. Docking onto chromatin via the Saccharomyces cerevisiae Rad9 Tudor domain. Yeast. 2007; 24:105–119. [PubMed: 17243194]
35. Huyen Y, et al. Methylated lysine 79 of histone H3 targets 53BP1 to DNA double-strand breaks. Nature. 2004; 432:406–411. [PubMed: 15525939]
36. Costelloe T, et al. The yeast Fun30 and human SMARCAD1 chromatin remodellers promote DNA end resection. Nature. 2012; 489:581–584. [PubMed: 22960744]
37. Chen X, et al. The Fun30 nucleosome remodeller promotes resection of DNA double-strand break ends. Nature. 2012; 489:576–580. [PubMed: 22960743]
38. Jazayeri A, McAinsh AD, Jackson SP. Saccharomyces cerevisiae Sin3p facilitates DNA double-strand break repair. Proc Natl Acad Sci U S A. 2004; 101:1644–1649. [PubMed: 14711989]
39. Bird AW, et al. Acetylation of histone H4 by Esa1 is required for DNA doublestrand break repair. Nature. 2002; 419:411–415. [PubMed: 12353039]
40. Miller KM, et al. Human HDAC1 and HDAC2 function in the DNA-damage response to promote DNA nonhomologous end-joining. Nat Struct Mol Biol. 2010; 17:1144–1151. [PubMed: 20802485]
41. Symington LS, Gautier J. Double-strand break end resection and repair pathway choice. Annu Rev Genet. 2011; 45:247–271. [PubMed: 21910633]
42. Ginsburg DS, Govind CK, Hinnebusch AG. NuA4 lysine acetyltransferase Esa1 is targeted to coding regions and stimulates transcription elongation with Gcn5. Mol Cell Biol. 2009; 29:6473–6487. [PubMed: 19822662]
43. Altaf M, et al. NuA4-dependent acetylation of nucleosomal histones H4 and H2A directly stimulates incorporation of H2A.Z by the SWR1 complex. J Biol Chem. 2010; 285:15966–15977. [PubMed: 20332092]
44. Raisner RM, et al. Histone variant H2A.Z marks the 5′ ends of both active and inactive genes in euchromatin. Cell. 2005; 123:233–248. [PubMed: 16239142]
45. Zhang H, Roberts DN, Cairns BR. Genome-wide dynamics of Htz1, a histone H2A variant that poises repressed/basal promoters for activation through histone loss. Cell. 2005; 123:219–231. [PubMed: 16239141]
46. Heo K, et al. FACT-mediated exchange of histone variant H2AX regulated by phosphorylation of H2AX and ADP-ribosylation of Spt16. Mol Cell. 2008; 30:86–97. [PubMed: 18406329]
47. Formosa T, et al. Defects in SPT16 or POB3 (yFACT) in Saccharomyces cerevisiae cause dependence on the Hir/Hpc pathway: polymerase passage may degrade chromatin structure. Genetics. 2002; 162:1557–1571. [PubMed: 12524332]
48. Biswas D, et al. A role for Chd1 and Set2 in negatively regulating DNA replication in Saccharomyces cerevisiae. Genetics. 2008; 178:649–659. [PubMed: 18245327]
49. Jin C, Felsenfeld G. Nucleosome stability mediated by histone variants H3.3 and H2A.Z. Genes Dev. 2007; 21:1519–1529. [PubMed: 17575053]
50. Adkins NL, Niu H, Sung P, Peterson CL. Nucleosome dynamics regulates DNA processing. Nat Struct Mol Biol. 2013; 20:836–842. [PubMed: 23728291]
51. Aguilera A. The connection between transcription and genomic instability. Embo J. 2002; 21:195–201. [PubMed: 11823412]
52. Gonzalez-Barrera S, Garcia-Rubio M, Aguilera A. Transcription and doublestrand breaks induce similar mitotic recombination events in Saccharomyces cerevisiae. Genetics. 2002; 162:603–614. [PubMed: 12399375]
53. Chai B, Huang J, Cairns BR, Laurent BC. Distinct roles for the RSC and Swi/Snf ATP-dependent chromatin remodelers in DNA double-strand break repair. Genes Dev. 2005; 19:1656–1661. [PubMed: 16024655]

54. Fnu S, et al. Methylation of histone H3 lysine 36 enhances DNA repair by nonhomologous end-joining. Proc Natl Acad Sci U S A. 2011; 108:540–545. [PubMed: 21187428]
55. Zentner GE, Henikoff S. Regulation of nucleosome dynamics by histone modifications. Nat Struct Mol Biol. 2013; 20:259–266. [PubMed: 23463310]
56. Chen J, Miller A, Kirchmaier AL, Irudayaraj JM. Single-molecule tools elucidate H2A.Z nucleosome composition. J Cell Sci. 2012; 125:2954–2964. [PubMed: 22393239]
57. Li B, et al. Preferential occupancy of histone variant H2AZ at inactive promoters influences local histone modifications and chromatin remodeling. Proc Natl Acad Sci U S A. 2005; 102:18385–18390. [PubMed: 16344463]
58. Lindsey-Boltz LA, Sancar A. RNA polymerase: the most specific damage recognition protein in cellular responses to DNA damage? Proceedings of the National Academy of Sciences of the United States of America. 2007; 104:13213–13214. [PubMed: 17684092]
59. Bermejo R, et al. The replication checkpoint protects fork stability by releasing transcribed genes from nuclear pores. Cell. 2011; 146:233–246. [PubMed: 21784245]
60. Raj A, van Oudenaarden A. Nature, nurture, or chance: stochastic gene expression and its consequences. Cell. 2008; 135:216–226. [PubMed: 18957198]
61. Aymard F, et al. Transcriptionally active chromatin recruits homologous recombination at DNA double-strand breaks. Nat Struct Mol Biol. 2014; 21:366–374. [PubMed: 24658350]
62. A histone H3K36 chromatin switch coordinates DNA double-strand break repair pathway choice. Nat Commun. 2014 P.
63. Morris SA, et al. Identification of histone H3 lysine 36 acetylation as a highly conserved histone modification. J Biol Chem. 2007; 282:7632–7640. [PubMed: 17189264]
64. Luco RF, Pan Q, Tominaga K, Blencowe BJ, Pereira-Smith OM, Misteli T. Regulation of alternative splicing by histone modifications. Science. 2010; 327:996–1000. [PubMed: 20133523]
65. Lawrence MS, et al. Discovery and saturation analysis of cancer genes across 21 tumour types. Nature. 2014; 505:495–501. [PubMed: 24390350]
66. Sweeney FD, Yang F, Chi A, Shabanowitz J, Hunt DF, Durocher D. Saccharomyces cerevisiae Rad9 acts as a Mec1 adaptor to allow Rad53 activation. Curr Biol. 2005; 15:1364–1375. [PubMed: 16085488]

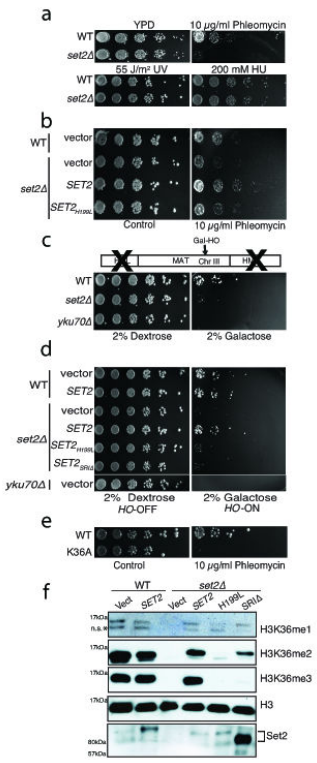

Fig 1. Methylation by Set2 at H3K36 and RNAPII–Set2 interaction is required for cellular resistance against double strand break (DSB)

Five-fold serial dilutions of over-night cultures (grown either in YPD or appropriate selection medium for plasmids) were spotted on indicated plates and pictures were taken after 2-4 days. For immunoblots, log phase cultures were used for preparing whole cell lysates as described in Experimental Procedures. (A) A *set2*Δ strain is sensitive to phleomycin but not to hydroxyurea and UV. (B) Sensitivity of *set2*Δ to DSB can be rescued by wild-type *SET2* but not by a catalytically dead ($SET2_{H199L}$) mutant. (C) *set2*Δ is sensitive to persistent Homothallic (HO) endonuclease-mediated DSB in the "donorless" strain JKM179. Schematic of the "donorless" strain is shown where the Gal-induced DSB is in the *MAT* locus of chromosome III. This strain has the *HML* and the *HMR* deleted and hence the DSB can be repaired only by NHEJ. (D) Rescue of *set2*Δ sensitivity to persistent DSB by wild-type *SET2* but not by a catalytically dead ($SET2_{H199L}$) or the SRIΔ mutant. (E) H3K36A phenocopies *set2*Δ on phleomycin. (F) Immunoblots showing the expression from the constructs used in Figs 1B and 1D. All the experiments were replicated at least three times.

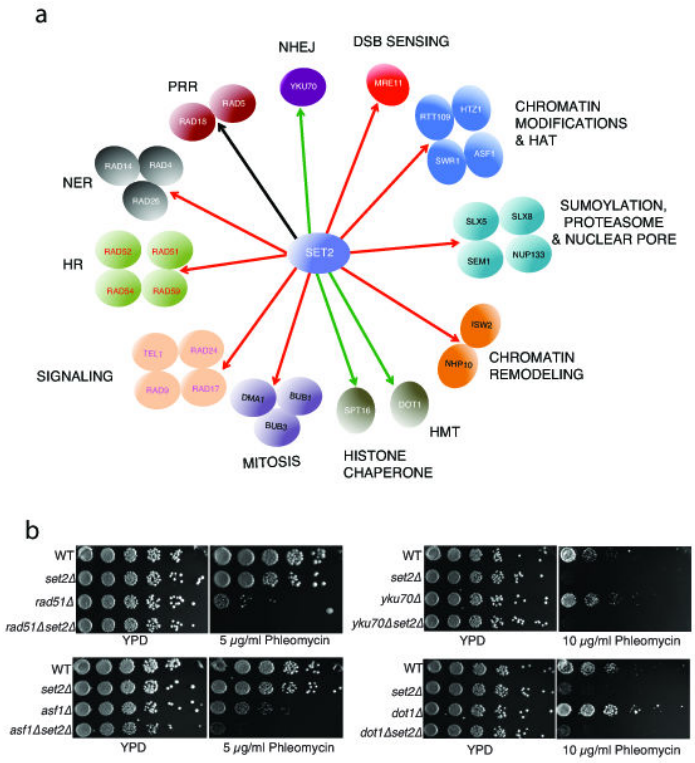

Fig 2. Genetic interaction of *SET2* with representative DNA damage response and repair genes

Representative DNA damage response and repair genes were selected from the Open Biosystems gene knockout collection and were verified by either phenotypic analysis or PCRs (using primers specific for the gene deletion) or both. Subsequent double mutants were made by gene replacement. (A) Qualitative representation of genetic interactions (on MMS) of *SET2* with DNA damage response and repair genes. Genes have been clustered together, manually, based on their annotated function in the *Saccharomyces* Genome Database (SGD). Black lines represent no genetic interaction, red lines indicate synthetic sick, and green lines indicate same pathway interaction. The entire screen was repeated twice. (B) Serial dilutions of representative strains show that *set2*Δ is sick with *rad51*Δ and *asf1*Δ while the *set2*Δ is epistatic to both *dot1*Δ and *yku70*Δ on phleomycin. Individual spotting assays were done in triplicate plates (at once) and the set of triplicates were repeated twice.

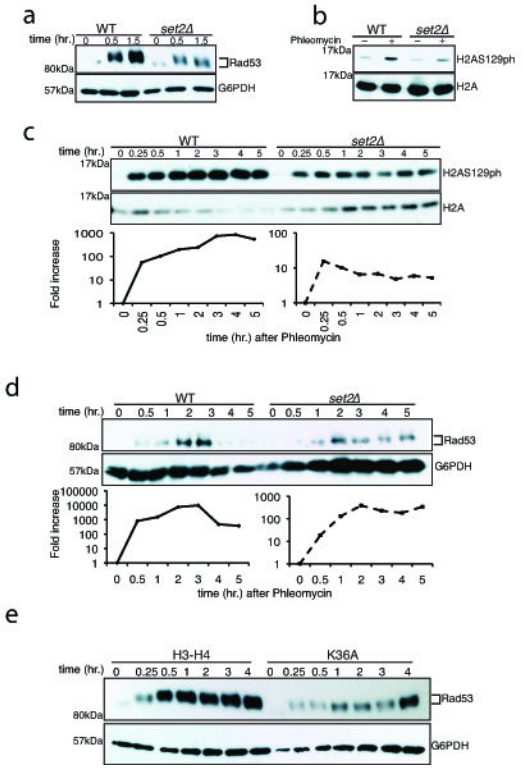

Fig 3. DNA damage signaling is attenuated in *set2*Δ

Log-phase cells were exposed to phleomycin for indicated times and whole cell extract was prepared (see Methods). (A) Diminution in Rad53 hyper-phosphorylation at indicated time-periods in a *set2*Δ after phleomycin treatment. The antibody to Rad53 is against the entire protein and G6PDH is used as a loading control. (B) Abrogated γ-H2A.X activation in *set2*Δ after phleomycin (50 μg/mL) treatment for two hours. (C) Time-course showing the activation of γ-H2A.X after phleomycin treatment. Quantification (H2AS129ph/H2A) of the Western blot is shown below. (D) Activation of Rad53 was monitored after phleomycin treatment in WT and *set2*Δ. Quantification (Rad53/G6PDH) of the Western blot is shown below, which reveals abrogated DNA damage checkpoint activation in *set2*Δ (plotted as a semi-log plot). (E) H3K36A mutant cells also show abrogated DNA damage checkpoint activation as monitored by Rad53 activation kinetics. Representative western blots, from at least 3 biological replicates), are presented.

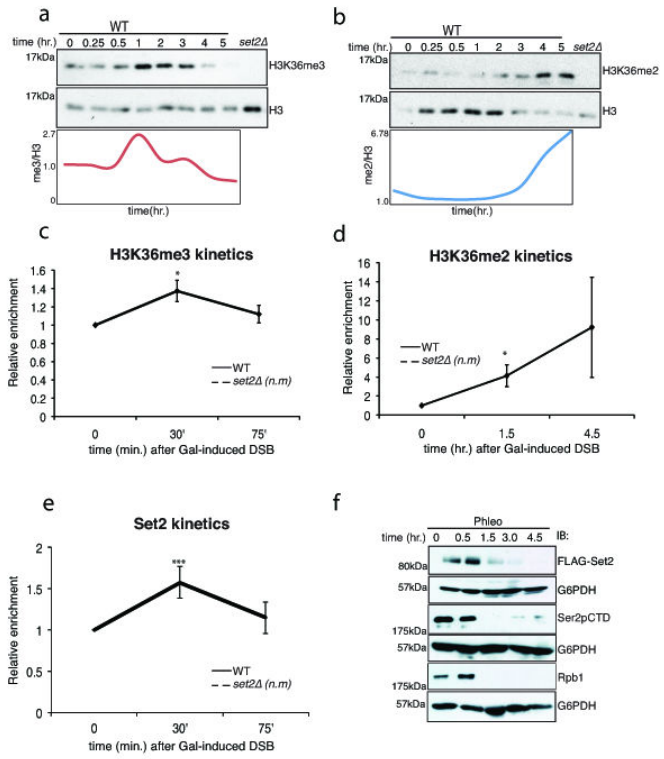

Fig 4. Temporal regulation of H3K36me3 and H3K36me2 correlates with proteasome-mediated degradation of Set2

Immunoblots showing the levels of (A) H3K36me3 and (B) H3K36me2 after DSB induction by phleomycin. Exponentially growing yeast cells were exposed to phleomycin for indicated times and whole cell extract was prepared. (C) H3K36me3 is transiently induced near the site of DSB (assessed by ChIP at 0.2 kb), at early time-points. The error bars represent ± s.e.m from two different biological replicates. n.m. represents 'not measurable' (D) H3K36me2 is induced near the site of DSB (assessed by ChIP at 0.2 kb), at later time points. The error bars represent ± s.e.m from two different biological replicates. n.m. represents 'not measurable' (* represents $p < 0.05$ for 4C and 4D). (E) Preferential enrichment of Set2 near DSB (assessed by ChIP at 0.2kb from DSB). n.m. represents not measurable (*** represents $p < 0.01$). (F) Time course experiment after phleomycin treatment for Set2 (FLAG-Set2), Ser2pCTD (elongating RNA Polymerase II) and Rpb1 (largest subunit of RNAPII). G6PDH is used as loading control.

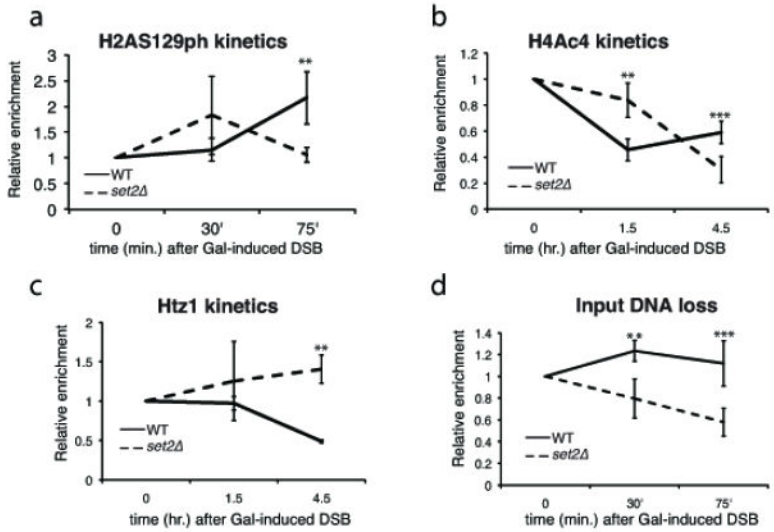

Fig 5. Set2 regulates chromatin remodeling after DSB induction

(A) Reduced γ-H2A.X levels in *set2*Δ by chip. (** represents p<0.03; error bars show ± s.e.m. from two independent biological replicates) (B) Altered kinetics of H4Ac4 at 0.2 kb from the DSB in *set2*Δ at indicated time points (** represents p <0.03 and *** represents p<0.01; error bars show ± s.e.m. from two independent biological replicates) (C) Increased Htz1 levels at 0.2 kb from the DSB in *set2*Δ (error bars represent mean ± s.d. from two independent biological replicates). (D) Increased loss of input DNA in *set2*Δ in G1-arrested cells at 1kb away from the DSB. (** represents p <0.03 and *** represents p<0.01; error bars show ± s.e.m. from two independent biological replicates).

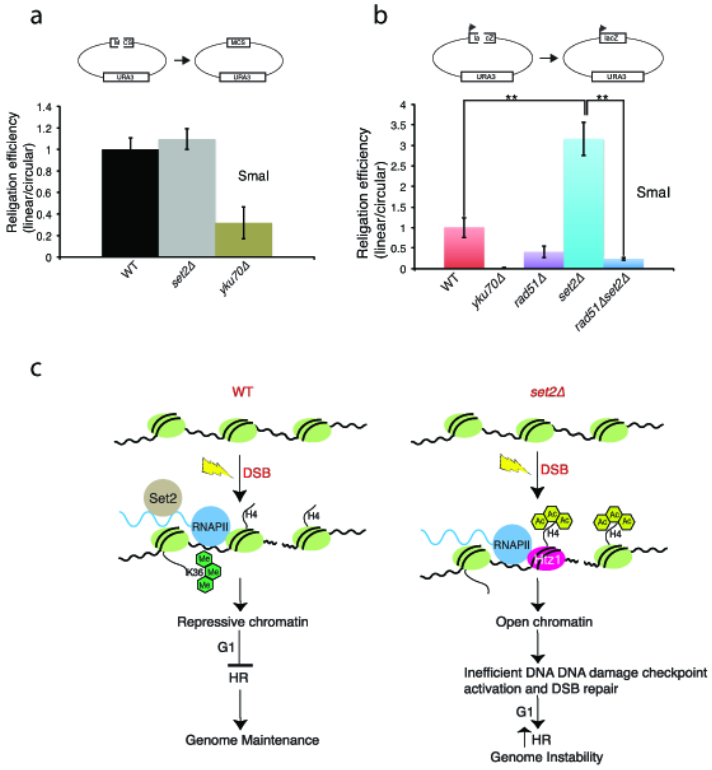

Fig 6. Set2 primarily functions in DSB repair in the context of a transcribing unit

(A) Linearized (SmaI) or circularized pRS316 plasmids were transformed, in parallel, into the indicated strains and colony numbers were counted after 2-3 days on Sc-Ura plates. Religation frequency was calculated as the ratio of the number of colonies obtained from linearized plasmid to the number colonies obtained from circularized plasmid, with the value for WT strain normalized to 1.0. *yku70*Δ is the positive control for the assay. (B) Linearized (SmaI) or circularized pGV255-live plasmids were transformed, in parallel, into indicated strains and number of colonies were counted after 2-3 days on Sc-Ura plates. Religation frequency was calculated as above. (** represents $p < 0.02$; error bars represent standard deviation from 3 different independent transformation experiments). (C) A simplified model depicting a function of Set2 and H3K36me in regulating DNA damage response and repair. Immediately after DSB (shown as 'lightning bolt'), Set2-dependent H3K36me3 becomes enriched around the DSB. Increased H3K36me3 ensures a de-acetylated chromatin structure to prevent inappropriate DNA transactions especially in the context of a transcription unit, which we propose is important for maintaining the genomic integrity of transcribing units. Consistent with this model, loss of Set2/H3K36me leads to abrogated DNA damage signaling activation, altered chromatin structure, and inappropriate repair.